Environmental Science & Technology

Article

pubs.acs.org/est

Investigation of Adsorption Behavior of Mercury on Au(111) from First Principles

Dong-Hee Lim, Shela Aboud, and Jennifer Wilcox*

Department of Energy Resources Engineering, Stanford University, 367 Panama Street, Green Earth Sciences, Stanford, California 94305-2220, United States

Supporting Information

ABSTRACT: The structural and electronic properties of Hg, SO_2, HgS, and HgO adsorption on Au(111) surfaces have been determined using density functional theory with the generalized gradient approximation. The adsorption strength of Hg on Au(111) increases by a factor of 1.3 (from −9.7 to −12.6 kcal/mol) when the number of surface vacancies increases from 0 to 3; however, the adsorption energy decreases with more than three vacancies. In the case of SO_2 adsorption on Au(111), the Au surface atoms are better able to stabilize the SO_2 molecule when they are highly undercoordinated. The SO_2 adsorption stability is enhanced from −0.8 to −9.3 kcal/mol by increasing the number of vacancies from 0 to 14, with the lowest adsorption energy of −10.2 kcal/mol at 8 Au vacancies. Atomic sulfur and oxygen precovered-Au(111) surfaces lower the Hg stability when Hg adsorbs on the top of S and O atoms. However, a cooperative effect between adjacent Hg atoms is observed as the number of S and Hg atoms increases on the perfect Au(111) surface, resulting in an increase in the magnitude of Hg adsorption. Details of the electronic structure properties of the Hg−Au systems are also discussed.

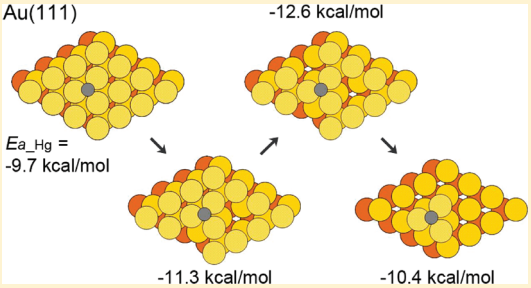

1. INTRODUCTION

The release of mercury (Hg) from coal combustion is of serious global concern.[1−3] Due to its toxicity, the U.S. Congress included mercury and its compounds in the 1990 Clean Air Act Amendments as a hazardous air pollutant. In December 2011, final standards were issued for limiting mercury, acid gases, and other toxic species from coal-fired power plants under the U.S. Environmental Protection Agency's (EPA's) Mercury and Air Toxics Standards (MATS) ruling.[4] Various sorbents or catalysts may be used in the combustion flue gas environment to capture and/or oxidize elemental Hg (Hg^0), including activated carbon, metal oxides, metal sulfides, and pure metals.[5−7] For coal gasification applications, transition and noble metals have been outlined as potential promising sorbents for Hg capture[2,8−11] in part because of their stability at high temperatures and their regeneration potential. These metals also have the potential to serve as Hg oxidation catalysts for coal combustion applications.

In particular, Au surfaces have been examined as a potential oxidation catalyst for Hg[2,11,12] since Au may be catalytically very active in the form of nanoparticles on suitable supports. According to a pilot-scale study of Hg oxidation in flue gas conducted by Blythe et al.,[13] although precious metal catalysts (Au or Pd) are high in cost, the cost difference between precious-metal catalysts and carbon-based sorbent catalysts is expected to be minimal due to the larger volume (44% more) requirements of the carbon-based materials. After 8 months of service, both Au- and Pd-based catalysts showed greater than 90% Hg oxidation, declining to 47 and 51% after 18 months, respectively. These catalysts have exhibited greater reactivity than selective catalytic reduction (SCR) catalysts (i.e., titanium/vanadium).

Although bulk gold surfaces are generally weakly active for most catalytic reactions due to its lack of a partially filled *d* band,[14,15] the catalytic reactivity of Au may be significantly enhanced through deposition onto various support materials, including oxide supports such as TiO_2, SiO_2, Fe_2O_3, Al_2O_3, MgO, and ZnO.[16−18] These supported heterogeneous gold catalysts have been intensively investigated,[19,20] in addition to enhanced catalytic reactivity sourced from highly reactive undercoordinated Au atoms, which is the case with SO_2 decomposition on undercoordinated Au(111).[21] Although the studies of supported and undercoordinated Au catalysts provide an understanding of the more realistic catalytic behavior, the investigation of single-crystal surfaces is also of importance for increasing understanding of fundamental mechanisms associated specifically with Au.

The oxidation of Hg in the flue gas occurs mainly by chlorinating species[2,11,12] such as HCl in the postcombustion environment, in which its concentration is on the order of hundreds of ppm, several orders of magnitude greater than Hg, which is on the order of ppb levels.[11] The interaction between Au and Cl has been widely investigated previously.[22−24] Besides

Received: January 24, 2012
Revised: May 24, 2012
Accepted: May 25, 2012
Published: May 25, 2012

dx.doi.org/10.1021/es300046d | Environ. Sci. Technol. 2012, 46, 7260−7266

the significant role of Cl in Hg oxidation on Au, sulfur and oxygen are also important factors on the Hg oxidation mechanism due to the S- and O-rich environment of the flue gas. Sulfur has a strong affinity for the Au(111) surface[25] and experimental and theoretical results show that atomic sulfur bound to Au(111) has a unique mobility (compared to other metals) that allows changes in adsorption-site coverage.[26] Also, oxygen adsorption can play a role in the Au surface reactivity. Experimental investigations show that atomic oxygen can release gold atoms from the Au(111) surface[27] and that clean Au surfaces exhibit chemical reactivity toward water when covered with atomic oxygen.[28]

The adsorption of electronegative species containing the elements Cl, S, and O has been found to significantly affect the morphology of the Au surface.[24] As indicated previously, gold in the presence of atomic S or O can undergo reconstruction by releasing gold atoms, thereby producing a higher density of undercoordinated Au sites.[29] A supported Au surface may contain enough defect sites to enhance the catalytic activity of Au for O_2 or SO_2[29] dissociation with the dissociated atoms likely occupying active surface sites because of the much larger concentration of these species in comparison to Hg^0 in the flue gas environment. For instance, SO_2 concentrations tend to be at ppm levels while Hg^0 concentrations are at the ppb level.[30] A possible mechanism of sulfur deposition on the Au surface is through decomposition pathways involving SO_2 and SO_3 followed by potentially bound elemental sulfide or oxidized sulfate species.[21] Understanding SO_2 adsorption on Au is necessary toward the elucidation of Hg oxidation on Au since sulfur may act to occupy binding sites for Hg as discussed in the Hg capture by activated carbon under varying conditions of SO_2 and SO_3 concentrations in the flue gas,[31] but may also provide a route for Hg adsorption via HgS compounds as discussed in the adsorption of Hg by Pd/Al_2O_3 in the presence of H_2S in the fuel gas.[32]

In the studies reported herein, density functional theory (DFT) methods have been applied to investigate the interaction between Hg and defective Au(111) surfaces. This was done as a first step toward understanding the Hg oxidation mechanism on gold surfaces, since it is well-known that Hg adsorbs to Au, Pt, and Pd surfaces,[11] appearing to react from an adsorbed state.[2,33−35] We also examine SO_2 binding on defective Au(111) surfaces and Hg−S and Hg−O interactions on clean Au(111) surfaces to determine how these species adsorb and potentially influence Hg adsorption. Details of the electronic properties of these investigated systems are also discussed.

2. COMPUTATIONAL METHODOLOGY

Density functional theory calculations were performed using the Vienna ab initio Simulation Package (VASP).[36−39] Ultrasoft Vanderbilt pseudopotentials[40] are used to describe core orbitals, and electron exchange correlation functionals were calculated using the Perdew and Wang[41] approximation (PW91) described by a generalized gradient approximation (GGA). The PW91 exchange-correlation functional has been known to provide a better description of Au−Au binding than Perdew−Burke−Ernzerhof (PBE) and revised-PBE (RPBE) functionals.[24] A plane-wave expansion with a cutoff of 350 eV was employed with a Methfessel and Paxton[42] Gaussian-smearing of order 2 with a width of 0.1 eV. Geometric relaxation was obtained with the conjugate-gradient (CG) algorithm until the forces on all the unconstrained atoms were less than 0.03 eV/Å. The surface Brillouin zone integration is calculated using 5 × 5 × 1 and 10 × 10 × 1 Monkhorst-Pack[43] k-point meshes for the Au(111)−$p(4 \times 4)$ and Au(111)−$p(2 \times 2)$ surfaces, respectively.

Scanning tunneling microscopy studies show that bare Au(111) surfaces form a $(22 \times \sqrt{3})R30°$ reconstruction resulting in a herringbone pattern.[44,45] Given that the energetic difference between the ideal (1 × 1) surface and the herringbone reconstruction is small, i.e., ∼0.02 eV per surface atom[45] and that the presence of several adsorbed molecules will lift the reconstruction, the simulated Au surface is modeled without the reconstruction.[46−48] The Au(111) surfaces were represented with an ideal four-layer slab and a 14.5 Å-thick vacuum region to prevent interactions between periodic images. The *xy*-plane is parallel to the surface and the *z*-axis is perpendicular to the surface. The bottom two layers are fixed at the equilibrium lattice constant, calculated through bulk energy minimization simulations, e.g., 4.18 Å, with the top two layers relaxed. A four-layer slab shows converged surface energy of 0.044 eV/Å^2 compared to that of a 20-layer slab (0.043 eV/Å^2) as described in Section 1 of the Supporting Information. This surface energy is consistent with a previous DFT study[24] reporting a surface energy of 0.044 eV/Å^2. Although the calculated surface energy is underestimated compared to the experimental value[49] of 0.0936 eV/Å^2, the PW91 functional shows improved accuracy compared to the PBE and RPBE functionals.[24]

The defective Au(111)−$p(4 \times 4)$ surfaces were modeled with 16 atoms in each layer and with a varying number of Au vacancies. A dipole correction associated with the asymmetric slab and the periodic boundary conditions[50,51] was incorporated and tested, but not included due to its negligible effect on adsorption energy (i.e., less than 0.08 kcal/mol or 4 meV for both Hg and SO_2 adsorption on defective Au surfaces with three and eight vacancies, respectively). The spin-polarized correction was also not taken into account because it had no substantial effect on Hg adsorption on the defective Au surface with three vacancies (i.e., less than 0.001 kcal/mol or 0.05 meV). Additionally, the defect-free Au(111)−$p(2 \times 2)$ surfaces with 4 atoms per surface were used to investigate the interaction of Hg with S and O atoms precovered on the defect-free surfaces. To validate the accuracy of the pseudopotentials, the bond length, dissociation energy, and harmonic vibrational frequency of an Hg dimer was calculated and compared against experimental data in previous work.[33,35]

The adsorption energies (E_{ads}) of Hg and SO_2 on defective Au(111)−$p(4 \times 4)$ surfaces are calculated as E_{ads} (Hg or SO_2) = $E_{Au+Adsorbate} - E_{Au} - E_{Adsorbate}$ where the three terms on the right-hand side represent the energy of the Au surface with the adsorbed Hg or SO_2, the energy of the Au surface, and the energy of gas-phase Hg or SO_2, respectively. The adsorption energy of Hg on S or O atoms precovered on defect-free Au surfaces are defined as E_{ads} (Hg) = $E_{Precovered+Adsorbate} - E_{Precovered} - E_{Adsorbate}$, where the first two terms on the right-hand side indicate the energy of the S or O precovered-Au surface with adsorbed Hg and the energy of the S or O precovered-Au surface, respectively. With this definition of adsorption energy, the more negative the energy, the stronger the interaction. The formation energy of an *n*-vacancy surface (E_{f_vac}) was evaluated as $E_{f\_vac} = E_{Au\_vac} - E_{ref} + nE_{bulk}$ where *n* is the number of the vacancy, E_{Au_vac} is the energy of Au(111) containing *n*-vacancies, E_{ref} is the energy of Au(111) with no vacancy, and E_{bulk} is the energy per Au atom in bulk.

dx.doi.org/10.1021/es300046d | Environ. Sci. Technol. 2012, 46, 7260−7266

3. RESULTS AND DISCUSSION

3.1. Hg Adsorption on Au(111). On the defect-free Au(111) surface with a Hg coverage of 0.0625 monolayer (ML), the 3-fold hollow site was found to be the most stable for Hg adsorption, but exhibited relatively weak physisorption energies of approximately −9.7 kcal/mol. As the number of vacancies surrounding the 3-fold hollow site increases, the strength of the interaction between Hg and Au increases as shown in Figure 1, but only up to three vacancies. When the top surface has three Au vacancies, the adsorption energy increases by a factor of 1.3, from −9.7 to −12.6 kcal/mol, but the adsorption energy decreases rapidly with more than 3 vacancies. This trend may be attributed to a favorable interaction between the Hg atom and the vacancy. One missing Au atom from the Au(111) surface creates a vacancy site or hexagonal hole (see Figure 1) thereby accumulating charge symmetrically around the edge of the hexagonal hole.[23] With more than 3 vacancies on the Au(111)−$p(4 \times 4)$ surface, the symmetry of the hexagonal hole is altered and the Au surface atoms form adatoms rather than the hexagonal hole. Due to a favorable interaction between the Hg atom and the vacancy site, the Hg atom relaxes toward the vacant hexagonal site resulting in shortening the distance between the Hg atom and the edge of the hexagonal site. For example, the shortest distances of the Hg−hexagonal site are 2.99 and 2.95 Å for surfaces with single vacancies at sites **b** and **c** as shown in Figure 1, respectively. With 3 vacancies, the shortest distance is 2.93 Å, indicating a stronger stability of Hg on the defective Au surface. To confirm these results, the stability of S and O atoms on the same defective Au surfaces was also examined. As shown in Section 2 of the Supporting Information, a similar trend was observed for both species, showing the highest adsorbate stability on surfaces in which 3 Au vacancies are present. Another similar adsorbate stabilization trend with increased surface vacancies was observed for Cl adsorption on Au(111).[23]

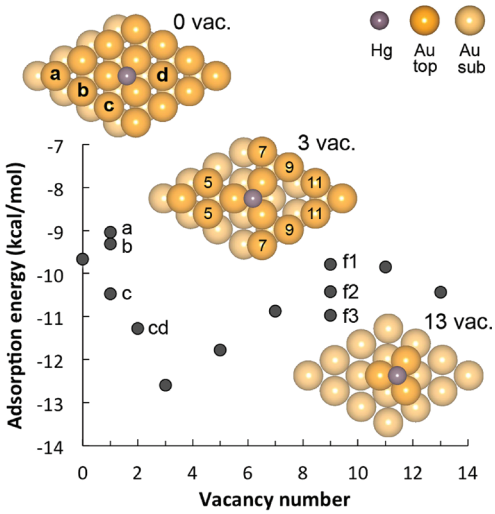

Figure 1. Effect of vacancies (vac.) on the stability of Hg on the Au(111)−$p(4 \times 4)$ surface. Dark purple, orange, and light orange colors represent Hg atom, the top layer of Au (Au top), and the second layer of Au (Au sub), respectively. The third and fourth layers of Au are omitted. Labels **a**, **b**, **c**, and **d** indicate one Au vacancy. Labels f1, f2, and f3 indicate different configurations of 9 vacancies. Numbers (n) of 5−11 shown in the 3-vacancy model represent Au atoms removed to create n vacancies (e.g., to create Au surfaces with 5 and 7 vacancies, two Au atoms numbered 5 and four Au atoms numbered 5 and 7 are removed, respectively). The configuration of 9 vacancies in the 3-vacancy model corresponds to f1.

The d-band of transition metals plays a central role in the adsorption process; more specifically, the position of the geometric mean of the d-band center relative to the Fermi level is a good measure of the relative reactivity of a given surface.[52,53] As the d-band center shifts upward to higher energies, the antibonding orbitals will become less available. The increased binding of Hg on defective Au surfaces can be understood through the shift in the surface d-band center of the undercoordinated Au adatoms. The d-band centers of the three Au atoms where Hg binds were examined for a clean Au (111) surface and a surface with 3 vacancies, which are −3.08 and −2.86 eV, respectively. As the surface d-band center shifts toward the Fermi level, the Au surface becomes more reactive resulting in an increase in stability of adsorbed Hg.

Interestingly, although the upward shift of the d-band center to higher energies serves as a good indicator of enhanced surface reactivity, the configurational arrangement of the surface atoms more significantly affects the stability of Hg on the Au surfaces. The Hg stability is relatively higher when the Au surface maintains the hexagonal vacancy, even though its d-band center of the surface is relatively lower, as shown in the Au surface examples of 3 and 9 vacancies in Section 3 of the Supporting Information. The Hg stability decreases as the symmetry of the hexagonal vacancy is disrupted. In addition, the formation energy of the vacancy (E_{f_vac}) (i.e., the energy required for bond cleavage to create a vacancy site) is likely to be associated with the trends of the Hg adsorption energy and the d-band center; however, the correlation is consistent only when the number of surface atoms is the same. For example, E_{f_vac} for three different Hg adsorption energies on Au with 9 vacancies (f1−f3) in Figure 1 are 3.54, 2.91, and 2.64 eV, respectively, and are subsequently inversely proportional to the Hg stability. However, E_{f_vac} for the three Au configurations with 3 vacancies are proportional to the Hg stability as shown in Section 3 of the Supporting Information. These observations indicate that the configurational arrangement of the Au surface atoms is a critical factor that significantly affects the Hg stability rather than E_{f_vac} and the d-band center.

The projected density of states (PDOS) of Hg adsorbed to the 3-fold hollow site of the (a) defect-free Au(111) surface and the (b) surface with 13 vacancies is shown in Figure 2. The d_{xz}, d_{yz} and d_{z^2} orbitals of Hg are all deeper in energy and less dispersed in the case of 13 vacancies (the d_{xz} is almost identical to the d_{yz}), which is consistent with stronger binding. A more pronounced interaction takes place between the Hg s-orbital and the d-band of the Au surface with vacancies, as is exhibited by the strong overlap in the DOS between −5 and −2 eV. The reduction in the coordination of the Au surface atoms allows for an enhanced interaction between the s- and d-orbitals of Hg with the s- and d-bands of Au creating a stronger interaction.

3.2. SO_2 Adsorption on Au(111). Figure 3 shows SO_2 binding on the Au(111) surfaces with vacancies. As shown, the Au surface atoms are better able to stabilize the SO_2 molecules when they are highly undercoordinated. All Au(111) surfaces with vacancies can exothermically bind SO_2. This result is supported by experimental observation of sulfur deposition on Au that is linked to the presence of highly reactive, undercoordinated Au atoms.[21] Interestingly, although the E_{f_vac} for Au surfaces with 2 vacancies (**ad** and **be** in Figure 3) are equivalent at 1.15 eV, SO_2 adsorption on the Au surface

dx.doi.org/10.1021/es300046d | Environ. Sci. Technol. 2012, 46, 7260−7266

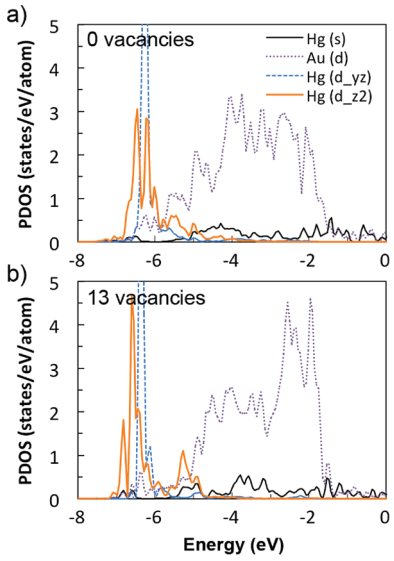

Figure 2. Projected density of states (PDOS) of *s*- and *d*-bands of Hg adsorbed on the Au(111)−$p(4 \times 4)$ surface with (a) 0 vacancies and (b) 13 vacancies with the Fermi energy referenced at 0 eV.

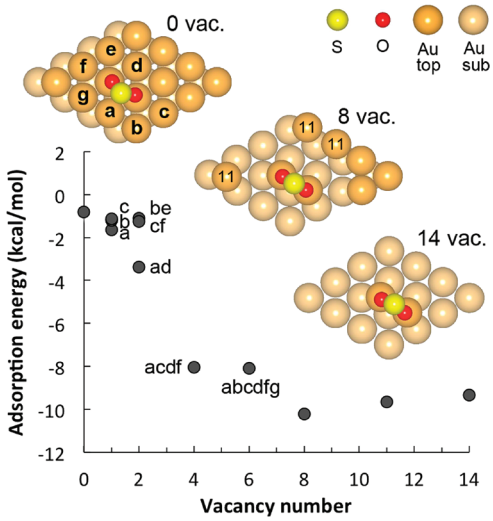

Figure 3. Effect of vacancies (vac.) on the stability of SO_2 molecule on the Au(111)−$p(4 \times 4)$ surface. Yellow, red, orange, and light orange colors represent S, O, the top layer of Au (Au top), and the second layer of Au (Au sub), respectively. The third and fourth layers of Au are omitted. Labels **a**, **b**, **c**, **d**, **e**, **f**, and **g** indicate one Au vacancy. More than two vacancies are formed in a combination among **a**−**g** vacancy sites. Number 11 in the 8-vacancy model represents Au atoms removed to create 11 vacancies.

with the **ad** vacancies (−3.4 kcal/mol) is three times more stable than that with the **be** vacancies (−1.1 kcal/mol). This is probably because the SO_2 molecule on the **ad** vacancy surface is directly exposed to the edge of the vacant hexagonal site that attracts adsorbates due to accumulated charge around the edge of the hexagonal site, similar to the case of Hg adsorption on the Au(111)−$p(4 \times 4)$ surface.

The adsorption configuration of SO_2 does significantly affect its adsorption energy with metals. For example, the adsorption energy of SO_2 varies on perfect Pt(111)−$p(3 \times 3)$ surfaces ranging from −1.7~−28.1 kcal/mol.[54] The most favorable configurations of adsorbed SO_2 may include a parallel configuration of SO_2 on Ir(111)[55] and a tilted configuration on Pt(111)[54] where the S atom and one of the O atoms are bound to the surface with the second O atom oriented to the vacuum space. In the current study, the tilted SO_2 configuration was the most favorable on the defective Au(111) surface with 14 vacancies (−12.9 kcal/mol, see Section 4 of the Supporting Information), but a vertical configuration in which two O atoms are interacting directly with the top Au atoms (−9.3 kcal/mol) as shown in Figure 3 was examined to facilitate computational calculations. Various configurations of SO_2 adsorption on the Au(111) surface with 14 vacancies are shown in Section 4 of the Supporting Information. Furthermore, cooperative effects due to neighboring SO_2−SO_2 interactions have also been shown to contribute to increasing the extent of sulfur deposition on Au surfaces experimentally,[46,56] but they are not taken into account in the current study.

Shown in Figure 4 is a plot of the PDOS for SO_2 on the Au(111)−$p(4 \times 4)$ surface with (a) 0 vacancies and (b) 8

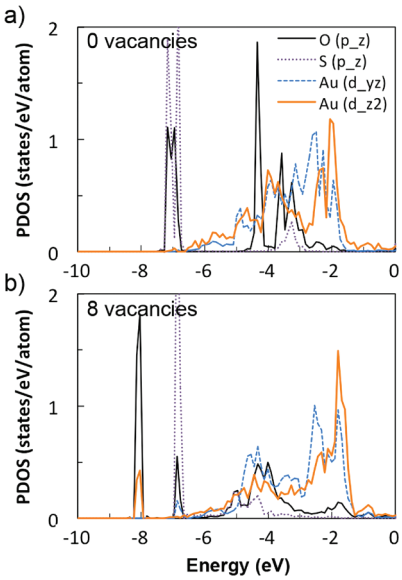

Figure 4. Projected density of states (PDOS) of SO_2 adsorbed on the Au(111)−$p(4 \times 4)$ surface with (a) 0 vacancies and (b) 8 vacancies with the Fermi energy referenced at 0 eV.

vacancies. The surface with 8 vacancies corresponds to the situation in which SO_2 binds to surface Au atoms with no nearest neighbors as shown in Figure 3. As the number of vacancies increases from 0 to 8, the adsorption energy increases from −0.8 to −10.2 kcal/mol. In this case, the electron density in the oxygen p_z orbital lies at approximately −8.0, −4.4, and −4.0 eV resulting in an enhanced interaction with the Au d_{z^2} orbitals leading to an overall more stable configuration. This interaction is primarily responsible for the SO_2 binding on the Au(111) surface.

3.3. Hg Interaction with S or O Precovered-Au(111) Surfaces. Considering the adsorption energies of atomic sulfur on Au(111) with 0.25 ML (−88.3 kcal/mol)[26] and atomic oxygen on Au(111) with 0.25 ML (−68.0 kcal/mol),[57] atomic S and O will adsorb more strongly to the stable 3-fold sites of Au(111) compared to Hg. To understand if the adsorbed S and O influences Hg adsorption, surface S and O coverages of 0.25 ML and 0.5 ML on a defect-free Au(111)−$p(2 \times 2)$ unit cell were modeled and the interaction of Hg with the S or O precovered-surface was investigated. The adsorption energies for the different surface configurations are presented in Table 1.

dx.doi.org/10.1021/es300046d | *Environ. Sci. Technol.* 2012, 46, 7260−7266

Table 1. Hg Interaction with S or O Atom Precovered on the Au(111)−$p(2 \times 2)$ Surface[a]

	diagram	Hg adsorption energy (kcal/mol per Hg)	
		X = S	X = O
0.25 ML HgX (3-fold hollow)		−1.49	−3.15
0.25 ML Hg + 0.50 ML X (3-fold hollow)		−1.75	−9.67
0.50 ML HgX (3-fold hollow)		−3.15	−9.67
0.25 ML HgX (top)		−3.54	−11.35
0.50 ML HgX (top)		−7.63	n/a

[a]Dark gray, yellow, and orange colors are Hg, X, and Au atoms, respectively, where X = S or O. The unit cell of $p(2 \times 2)$ is shown by a rhombus in black ("n/a" indicates that the O precovered-Au surface is not available).

Overall, when Hg adsorbs on the top sites of S and O atoms, the Hg stability is lower compared to the vacancy-free Au(111)−$p(4 \times 4)$ surface (−9.7 kcal/mol) shown in Figure 1. Additionally, Hg adsorption in parallel with atomic S on a $p(4 \times 4)$ surface was investigated as shown in Section 5 of the Supporting Information. This result indicates that each Hg and S atom adsorbs separately at 3-fold hollow sites and that the Hg stability (−8.9 kcal/mol per Hg) is also slightly lower than that of the clean Au surface.

As the amount of atomic S (or O) and Hg increases on the defect-free Au(111) surface, the adsorption energy of Hg increases, suggesting a cooperative effect between adjacent Hg atoms. Previous studies have confirmed that lateral Hg−Hg interactions are favorable on Cu(001),[10] Cu(100),[58] and Ni(100).[59] When Hg coverage increases from 0.125 to 0.5 ML by changing a Cu(001)−$c(4 \times 4)$ surface to a $c(2 \times 2)$ surface, the weak attractive Hg−Hg interaction gains a small energetic advantage of 0.9 kcal/mol; however, a Cu(001)−$c(1 \times 1)$ surface with a Hg coverage of 1.0 ML leads to a repulsive lateral Hg−Hg interaction at Hg−Hg distances less than 2.6 Å.[10] In the current study it has been found that the Hg−Hg interaction on the S precovered-Au(111) surface is energetically favored by 1.7 and 4.1 kcal/mol per Hg when coverage is increased from 0.25 to 0.5 ML at the 3-fold hollow and top sites, respectively. The nearest Hg−Hg distance at 0.5 ML coverages at the 3-fold hollow and top sites is 3.41 and 2.95 Å, respectively. It should be also noted that the behavior of Hg adsorption on hollow sites of clean Au(111) surfaces was reported differently, resulting in lower Hg stability at higher coverage (i.e., −8.8 kcal/mol for 0.25 ML and −8.1 kcal/mol for 0.5 ML).[10] In the current investigation, this discrepancy might be attributed to an effect associated with atomic S precovering the Au surface. In the case of the Hg−Hg interaction on the atomic O precovered-Au(111) surface, a similar trend is observed as in the atomic S precovered-Au(111) surface, but with an increased attractive Hg−Hg interaction as indicated in Table 1.

On the other hand, when Hg adsorbs in a parallel configuration with atomic S on a $p(4 \times 4)$ surface, the Hg stability becomes lower with increasing Hg coverage from 0.0625 to 0.125 ML (i.e., from −8.9 to −5.0 kcal/mol per Hg), as described in Section 5 of the Supporting Information. This is due to the fact that each Hg and S atom separately adsorbs at 3-fold hollow sites on a larger surface, resulting in a Hg−Hg distance of 6.40 Å, which is too long and in general results in a negative effect of adsorbate coverage on Hg adsorption[10,26,57] (i.e., the adsorbate becomes less stable as its coverage increases).

Note that in Table 1 the Hg adsorption energy of 0.25 ML HgX (where X = S or O) at the top site is lower (more stable) than that at the 3-fold hollow site. Because atomic S and O adsorb more strongly to the 3-fold hollow sites of Au(111) than other surface sites,[26,57] the Au surface precovered with atomic S (or O) at its top site is relatively much less stable (higher energy) compared to the Au surface with atomic S (or O) at the 3-fold hollow site. This results in increased Hg stability as the Hg atom interacts directly with the S (or O) atom adsorbed at the top site of Au. Additionally, adsorption energies of an HgS molecule (without precovered species) for the 0.25 ML HgX systems of Table 1 are −64.5 and −36.9 kcal/mol at the 3-fold hollow and the top sites, respectively. This indicates that the 3-fold hollow site of Au(111) is a more favorable adsorption site than the top site.

Figure 5 shows the PDOS for HgS (a) and HgO (b) on the top site of the Au(111)−$p(2 \times 2)$ surface with a coverage of 0.25 ML. In Figure 5a, the peak at approximately −11.6 eV corresponds to the bonding interaction between the Au *d*-orbital and S *s*-orbital. The S *p*-orbitals are strongly hybridized with the Au *d*-orbitals and shifted to the lower energy level, which is primarily responsible for the binding of HgS with S bound directly to the Au surface. Also, comparing to the Hg *d*-

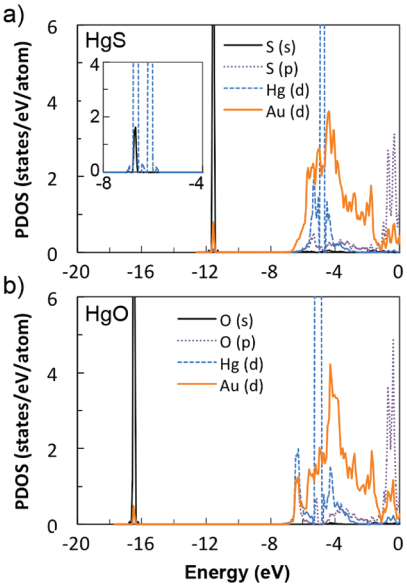

Figure 5. Projected density of states (PDOS) of (a) HgS and (b) HgO adsorbed on the Au top site of the Au(111)−$p(2 \times 2)$ surface with the Fermi energy referenced at 0 eV. The inset presents the Hg *d*-orbital and S *s*-orbital of a gas-phase HgS molecule.

dx.doi.org/10.1021/es300046d | Environ. Sci. Technol. 2012, 46, 7260−7266

orbital of a gas-phase HgS molecule in the inset of Figure 5a, the *d*-orbital of Hg interacting with the Au surface is hybridized with the *d*-orbital of Au between approximately −6 and −3 eV. This contributes to the stability of the HgS molecule on the Au surface. Furthermore, the interaction of HgO on the Au(111) surface is similar to the interactions for HgS. In Figure 5b, as compared to Figure 5a, the peak corresponding to the HgO interaction is much deeper at approximately −16.5 eV. The Hg *d*-orbital hybridization of HgO with the Au *d*-orbital is stronger, more broadened, and more shifted to the lower energy level than that of HgS, which is responsible for the stronger Hg−O interaction than the Hg−S on the Au surface as shown in Table 1.

For environmental technology implications, the current work serves as a first step to providing insight on the behavior of Hg on defective gold, which will facilitate the investigation of mechanisms associated with Hg oxidation pathways for the design of effective Hg control technologies. The current work may be applicable to not only Hg oxidation that takes place from adsorbed Hg species, but also Hg capture through the formation of Hg−Au amalgams,[60] which require an initial monolayer of chemisorbed Hg on the Au surface along with adequate Hg partial pressure. For example, according to the stability of Hg adsorbed on defective Au(111) surfaces with varying number of vacancies, it will be important to recognize that a proper number of Au vacancies is necessary for maximizing Hg uptake on these materials. To promote Hg removal by using Hg oxidation, however, a balance in the Hg adsorption strength may be necessary to provide stable binding of Hg for initial oxidation while still allowing for the desorption of oxidized Hg species to the gas phase for capture downstream in existing control devices such as wet flue gas desulfurization units. This balance may be introduced when gold surfaces are precovered with atomic S and O species according to the current study. The future work should investigate the oxidation pathways via O_2 or halogenation for downstream Hg capture in a wet scrubber.

■ ASSOCIATED CONTENT

Supporting Information

Details of the surface energies of Au(111), adsorption of atomic S and O on the Au(111)−$p(4 \times 4)$ surface, factors affecting Hg adsorption on the Au(111)−$p(4 \times 4)$ surface with 3 and 9 vacancies, adsorption of SO_2 on the Au(111)−$p(4 \times 4)$ surface with 14 vacancies, and Hg adsorption in parallel with atomic S on the defect-free Au(111)−$p(4 \times 4)$ surface. This material is available free of charge via the Internet at http://pubs.acs.org.

■ AUTHOR INFORMATION

Corresponding Author

*E-mail: wilcoxj@stanford.edu; phone: (650) 724-9449; fax: (650) 725-2099.

Notes

The authors declare no competing financial interest.

■ ACKNOWLEDGMENTS

We thank the Electric Power Research Institute for making this research possible through their mercury research funding to the Clean Energy Conversions Laboratory at Stanford University. The computational resources were supported by the National Science Foundation through TeraGrid resources provided by Texas Advanced Computing Center (TACC) and in part by the supercomputing cluster of the Center for Computational Earth & Environmental Science at Stanford University.

■ REFERENCES

(1) Guo, X.; Zheng, C. G.; Xu, M. H. Characterization of mercury emissions from a coal-fired power plant. *Energy Fuels* **2007**, *21* (2), 898−902.

(2) Presto, A. A.; Granite, E. J. Survey of catalysts for oxidation of mercury in flue gas. *Environ. Sci. Technol.* **2006**, *40* (18), 5601−5609.

(3) Presto, A. A.; Granite, E. J.; Karash, A.; Hargis, R. A.; O'Dowd, W. J.; Pennline, H. W. A kinetic approach to the catalytic oxidation of mercury in flue gas. *Energy Fuels* **2006**, *20* (5), 1941−1945.

(4) U.S. Environmental Protection Agency. *National Emission Standards for Hazardous Air Pollutants From Coal- and Oil-Fired Electric Utility Steam Generating Units and Standards of Performance for Fossil-Fuel-Fired Electric Utility, Industrial-Commercial-Institutional, and Small Industrial-Commercial-Institutional Steam Generating Units; Proposed Rule*; United States Environmental Protection Agency; Federal Register, Vol. *76*, No. 85: 2011.

(5) Monnell, J. D.; Vidic, R. D.; Gang, D.; Karash, A.; Granite, E. J. Recent Advances in Trace Metal Capture Using Micro and Nano-Scale Sorbents. In *Proceedings of the 23rd Pittsburgh Coal Conference, Pittsburgh, PA*, 2006.

(6) Granite, E. J.; Pennline, H. W.; Hargis, R. A. Novel sorbents for mercury removal from flue gas. *Ind. Eng. Chem. Res.* **2000**, *39* (4), 1020−1029.

(7) Wilcox, J.; Rupp, E.; Ying, S. C.; Lim, D.-H.; Negreira, A. S.; Kirchofer, A.; Feng, F.; Lee, K. Mercury adsorption and oxidation in coal combustion and gasification processes. *Int. J. Coal Geol.* **2012**, *90*, 4−20.

(8) Poulston, S.; Granite, E. J.; Pennline, H. W.; Myers, C. R.; Stanko, D. P.; Hamilton, H.; Rowsell, L.; Smith, A. W. J.; Ilkenhans, T.; Chu, W. Metal sorbents for high temperature mercury capture from fuel gas. *Fuel* **2007**, *86* (14), 2201−2203.

(9) Granite, E. J.; Myers, C. R.; King, W. P.; Stanko, D. C.; Pennline, H. W. Sorbents for mercury capture from fuel gas with application to gasification systems. *Ind. Eng. Chem. Res.* **2006**, *45* (13), 4844−4848.

(10) Steckel, J. A. Density functional theory study of mercury adsorption on metal surfaces. *Phys. Rev. B* **2008**, *77* (11), 115412.

(11) Presto, A. A.; Granite, E. J. Noble Metal Catalysts for Mercury Oxidation in Utility Flue Gas: Gold, Palladium and Platinum Formulations. *Platinum Met. Rev.* **2008**, *52* (3), 144−154.

(12) Zhao, Y. X.; Mann, M. D.; Pavlish, J. H.; Mibeck, B. A. F.; Dunham, G. E.; Olson, E. S. Application of gold catalyst for mercury oxidation by chlorine. *Environ. Sci. Technol.* **2006**, *40* (5), 1603−1608.

(13) Blythe, G.; Dombrowski, K.; Machalek, T.; Richardson, C.; Richardson, M. *Pilot Testing of Mercury Oxidation Catalysts for Upstream of Wet FGD Systems, Final Report*; Cooperative Agreement DE-FC26-01NT41185; EPRI: Palo Alto, CA, and U.S. Department of Energy, National Energy Technology Laboratory: Pittsburgh, PA, 2006.

(14) Bond, G. C.; Thompson, D. T. Gold-catalysed oxidation of carbon monoxide. *Gold Bull.* **2000**, *33* (2), 41−51.

(15) Cant, N. W.; Hall, W. K. Catalytic oxidation. IV. Ethylene and propylene oxidation over gold. *J. Phys. Chem.* **1971**, *75* (19), 2914−2921.

(16) Rodriguez, J. A.; Liu, P.; Vines, F.; Illas, F.; Takahashi, Y.; Nakamura, K. Dissociation of SO_2 on Au/TiC(001): Effects of Au-C interactions and charge polarization. *Angew. Chem.-Int. Ed.* **2008**, *47* (35), 6685−6689.

(17) Lin, S. D.; Bollinger, M.; Vannice, M. A. Low-temperature CO oxidation over Au/TiO_2 and Au/SiO_2 catalysts. *Catal. Lett.* **1993**, *17* (3−4), 245−262.

(18) Haruta, M. Size- and support-dependency in the catalysis of gold. *Catal. Today* **1997**, *36* (1), 153−166.

(19) Corti, C. W.; Holliday, R. J.; Thompson, D. T. Progress towards the commercial application of gold catalysts. *Top. Catal.* **2007**, *44* (1−2), 331−343.

(20) Carabineiro, S. A. C.; Nieuwenhuys, B. E. Reactions of small molecules on gold single crystal surfaces. *Gold Bull.* **2010**, *43* (4), 252−266.
(21) Biener, M. M.; Biener, J.; Friend, C. M. Enhanced transient reactivity of an O-sputtered Au(111) surface. *Surf. Sci.* **2005**, *590* (2−3), L259−L265.
(22) Gao, W. W.; Baker, T. A.; Zhou, L.; Pinnaduwage, D. S.; Kaxiras, E.; Friend, C. M. Chlorine adsorption on Au(111): Chlorine overlayer or surface chloride? *J. Am. Chem. Soc.* **2008**, *130* (11), 3560−3565.
(23) Baker, T. A.; Friend, C. M.; Kaxiras, E. Chlorine interaction with defects on the Au(111) surface: A first-principles theoretical investigation. *J. Chem. Phys.* **2008**, *129* (10), 104702.
(24) Baker, T. A.; Friend, C. M.; Kaxiras, E. Effects of chlorine and oxygen coverage on the structure of the Au(111) surface. *J. Chem. Phys.* **2009**, *130* (8), 084701.
(25) Gottschalck, J.; Hammer, B. A density functional theory study of the adsorption of sulfur, mercapto, and methylthiolate on Au(111). *J. Chem. Phys.* **2002**, *116* (2), 784−790.
(26) Rodriguez, J. A.; Dvorak, J.; Jirsak, T.; Liu, G.; Hrbek, J.; Aray, Y.; Gonzalez, C. Coverage effects and the nature of the metal-sulfur bond in S/Au(111): High-resolution photoemission and density-functional studies. *J. Am. Chem. Soc.* **2003**, *125* (1), 276−285.
(27) Min, B. K.; Deng, X.; Pinnaduwage, D.; Schalek, R.; Friend, C. M. Oxygen-induced restructuring with release of gold atoms from Au(111). *Phys. Rev. B* **2005**, *72* (12), 121410.
(28) Kim, T. S.; Gong, J.; Ojifinni, R. A.; White, J. M.; Mullins, C. B. Water activated by atomic oxygen on Au(111) to oxidize CO at low temperatures. *J. Am. Chem. Soc.* **2006**, *128* (19), 6282−6283.
(29) Min, B. K.; Alemozafar, A. R.; Biener, M. M.; Biener, J.; Friend, C. M. Reaction of Au(111) with sulfur and oxygen: Scanning tunneling microscopic study. *Top. Catal.* **2005**, *36* (1−4), 77−90.
(30) Hutson, N. D.; Krzyzynska, R.; Srivastava, R. K. Simultaneous removal of SO_2, NO_x, and Hg from coal flue gas using a $NaClO_2$-enhanced wet scrubber. *Ind. Eng. Chem. Res.* **2008**, *47* (16), 5825−5831.
(31) Presto, A. A.; Granite, E. J. Impact of sulfur oxides on mercury capture by activated carbon. *Environ. Sci. Technol.* **2007**, *41* (18), 6579−6584.
(32) Baltrus, J. P.; Granite, E. J.; Pennline, H. W.; Stanko, D.; Hamilton, H.; Rowsell, L.; Poulston, S.; Smith, A.; Chu, W. Surface characterization of palladium-alumina sorbents for high-temperature capture of mercury and arsenic from fuel gas. *Fuel* **2010**, *89* (6), 1323−1325.
(33) Sasmaz, E.; Aboud, S.; Wilcox, J. Hg binding on Pd binary alloys and overlays. *J. Phys. Chem. C* **2009**, *113* (18), 7813−7820.
(34) Sasmaz, E.; Wilcox, J. Mercury species and SO_2 adsorption on CaO(100). *J. Phys. Chem. C* **2008**, *112* (42), 16484−16490.
(35) Aboud, S.; Sasmaz, E.; Wilcox, J. Mercury adsorption on PdAu, PdAg and PdCu alloys. *Main Group Chem.* **2008**, *7* (3), 205−215.
(36) Kresse, G.; Hafner, J. Ab initio molecular dynamics for liquid metals. *Phys. Rev. B* **1993**, *47* (1), 558−561.
(37) Kresse, G.; Hafner, J. Ab initio molecular-dynamics simulation of the liquid-metal-amorphous-semiconductor transition in germanium. *Phys. Rev. B* **1994**, *49* (20), 14251−14269.
(38) Kresse, G.; Furthmüller, J. Efficient iterative schemes for ab initio total-energy calculations using a plane-wave basis set. *Phys. Rev. B* **1996**, *54* (16), 11169−11186.
(39) Kresse, G.; Furthmüller, J. Efficiency of ab-initio total energy calculations for metals and semiconductors using a plane-wave basis set. *Comput. Mater. Sci.* **1996**, *6* (1), 15−50.
(40) Vanderbilt, D. Soft self-consistent pseudopotentials in a generalized eigenvalue formalism. *Phys. Rev. B* **1990**, *41* (11), 7892.
(41) Perdew, J. P.; Wang, Y. Accurate and simple analytic representation of the electron-gas correlation energy. *Phys. Rev. B* **1992**, *45* (23), 13244.
(42) Methfessel, M.; Paxton, A. T. High-precision sampling for Brillouin-zone integration in metals. *Phys. Rev. B* **1989**, *40* (6), 3616−3621.
(43) Monkhorst, H. J.; Pack, J. D. Special points for Brillouin-zone integrations. *Phys. Rev. B* **1976**, *13* (12), 5188−5192.
(44) Chen, W.; Madhavan, V.; Jamneala, T.; Crommie, M. F. Scanning tunneling microscopy observation of an electronic superlattice at the surface of clean gold. *Phys. Rev. Lett.* **1998**, *80* (7), 1469−1472.
(45) Wang, Y.; Hush, N. S.; Reimers, J. R. Simulation of the Au(111)-$(22\times\sqrt{3})$ surface reconstruction. *Phys. Rev. B* **2007**, *75* (23), 233416.
(46) Biener, M. M.; Biener, J.; Friend, C. M. Revisiting the S−Au(111) interaction: Static or dynamic. *Langmuir* **2005**, *21* (5), 1668−1671.
(47) Ibach, H.; Bach, C. E.; Giesen, M.; Grossmann, A. Potential-induced stress in the solid-liquid interface: Au(111) and Au(100) in an $HClO_4$ electrolyte. *Surf. Sci.* **1997**, *375* (1), 107−119.
(48) Sander, D.; Linke, U.; Ibach, H. Adsorbate-induced surface stress - sulfur, oxygen and carbon on Ni(100). *Surf. Sci.* **1992**, *272* (1−3), 318−325.
(49) Boer, F. R.; Boom, R.; Mattens, W. C. M.; Miedema, A. R.; Niessen, A. K. *Cohesion in Metals: Transition Metal Alloys*; North-Holland: Amsterdam, Oxford, New York, Tokyo, 1988.
(50) Makov, G.; Payne, M. C. Periodic boundary conditions in ab initio calculations. *Phys. Rev. B* **1995**, *51* (7), 4014−4022.
(51) Neugebauer, J.; Scheffler, M. Adsorbate-substrate and adsorbate-adsorbate interactions of Na and K adlayers on Al(111). *Phys. Rev. B* **1992**, *46* (24), 16067−16080.
(52) Hammer, B.; Nørskov, J. K. Electronic factors determining the reactivity of metal surfaces. *Surf. Sci.* **1995**, *343* (3), 211−220.
(53) Hammer, B.; Nørskov, J. K., Theoretical surface science and catalysis - Calculations and concepts. In *Advances in Catalysis, Vol 45*; Academic Press Inc: San Diego, CA, 2000; Vol. *45*, pp 71−129.
(54) Lin, X.; Hass, K. C.; Schneider, W. F.; Trout, B. L. Chemistry of sulfur oxides on transition metals I: Configurations, energetics, orbital analyses, and surface coverage effects of SO_2 on Pt(111). *J. Phys. Chem. B* **2002**, *106* (48), 12575−12583.
(55) Jiang, R.; Guo, W.; Li, M.; Zhu, H.; Li, J.; Zhao, L.; Fu, D.; Shan, H. Density Functional Study of the Reaction of SO(2) on Ir(111). *J. Phys. Chem. C* **2009**, *113* (42), 18223−18232.
(56) Biener, M. M.; Biener, J.; Friend, C. M. Sulfur-induced mobilization of Au surface atoms on Au(111) studied by real-time STM. *Surf. Sci.* **2007**, *601* (7), 1659−1667.
(57) Okazaki-Maeda, K.; Kohyama, M. Atomic oxygen adsorption on Au(100) and Au(111): Effects of coverage. *Chem. Phys. Lett.* **2010**, *492* (4−6), 266−271.
(58) Kime, Y. J.; Zhang, J. D.; Dowben, P. A. Lateral interactions and structural phase-transitions in ultrathin Hg films. *Surf. Sci.* **1992**, *268* (1−3), 98−112.
(59) Jones, R. G.; Tong, A. W. L. Mercury adsorption on NI(100). *Surf. Sci.* **1987**, *188* (1−2), 87−106.
(60) Butler, M. A.; Ricco, A. J.; Baughman, R. J. Hg adsorption on optically thin Au films. *J. Appl. Phys.* **1990**, *67* (9), 4320−4326.